Alteration of Bentonite From Ughelli By Nitric Acid Activation: Kinetics And Physicochemical Properties

R. O. Ajemba

Department of Chemical Engineering, Nnamdi Azikiwe University, P. M. B. 5025*, Awka, Anambra, Nigeria*
ginaajemba@rocketmail.com

Abstract

The physicochemical properties of Ughelli bentonite was modified by nitric acid activation to improve its performance. The bentonite mineral was reacted with different concentrations of nitric acid ranging from 2 to 16 mol.L^{-1}. The reactions were performed at different times and temperatures to study the process kinetics. The chemical composition and physical characteristics of the natural and treated samples were analyzed. To investigate the adsorptive performance of the modified samples, they were used to bleach soya bean oil. The surface area and adsorption capacity increased from 117.6 $m^2.g^{-1}$ to 364 $m^2.g^{-1}$ and 29 to 95 %, respectively, after activating with 14 mol.L^{-1} of HNO_3. Kinetics studies showed that the activation process were controlled by the chemical reaction step and can be given by: $1 - (1 - X)^{1/3} = k\,t$; where X is the fraction of the cations removed at time t. This study has proved that bentonite from Ughelli can be modified by nitric acid activation to increase its performance as adsorbent in the vegetable oil purification industry.

Keywords: Physicochemical, Ughelli betonite

1. Introduction

Acid modified natural bentonites are the subject of many studies (Taha et al., 2011; Dias et al., 2003; Tomic et al., 2011; Bergaya and Lagaly, 2001; Carrado and Komadel, 2009; Madejova et al., 2009; Amari et al., 2010). The acid treatment of clay minerals is referred to as acid activation because it increases the specific surface area and number of active sites of the solids. This treatment modifies the surfaces of clays by dis-aggregations of particles, possible elimination of mineral impurities and removal of metal-exchange cations (Dias et al., 2003). The first step in modifying the clay mineral structure with acid is a separation of exchangeable cations from protons. The second step is flushing Al, Mg, and Fe from octahedral and tetrahedral sheets, in the way that SiO_4 groups of tetrahedral sheets remain mostly intact. Increasing of the surface area is an important physical change (Kheok and Lim, 1982; Morgan et al., 1985; Taylor et al., 1989; Rhodes and Brown, 1992; Christidis et al., 1997; Komadel, 2003) which is a function of the structure and removal of octahedral sheets (Madejova et al., 1998; Komadel and Madejova, 2006; Tyagi et al., 2006).

The common commercial use of acid-activated clay minerals is bleaching or de-colourations of oils (Srasra et al, 1989) and in general in the field of adsorption and catalysis (Fahn and Fenderl, 1983; Mokaya and Jones, 1995). Acid treated clay minerals are commercially used for the bleaching or decolourizing of oils because they exhibit wide range of chemical and physical properties depending on the extent of activation (Boki et al., 1992). Acid activation of palygorskite revealed an important increase in the specific surface area (Vicente et al., 1995) and increase in the number of acid centers and destruction of the silicate structure was also observed during the activation of a ferrous saponite (Vicente et al, 1996). These facts lead to the conclusion that, for a particular clay mineral, bleaching earth properties such as surface area and acidity should be optimized by properly controlling the activation conditions such as type and amount of acid, temperature, and treatment time (Breen et al, 1997; Falaras et al, 1999).

From the older studies of Osthaus (1954 and 1956) and Abdul-Latif and Weaver (1969) to recent papers authors have studied the dissolution processes of silicates from the kinetic aspects, especially for Mg (II) cations, showing that the diffusion of the protons into the pores with planar or cylindrical geometries is the limiting step of the reaction. Indeed, when this process has taken over, the chemical reaction becomes instantaneous, being of first-order with respect to the metal cation and acid concentration.

The purpose of the present study is to investigate the chemical composition, cation exchange capacity, surface area, and adsorption capacity as a function of nitric acid treatment of bentonite from Ughelli. Also, a kinetic model has been applied to the data from the analysis of the liquids obtained after washing the different solid residues from activation reactions.

2. Experimental Procedure

2.1 Activation of the raw bentonite

The clay sample was dried, grinded and sieved to 0.075 mm particle size. The sized samples were reacted with different concentrations (2, 4, 8, 12, 14, and 16 mol/l) of nitric acid solution in the following manner. 10 g of the sized fraction was weighed out and reacted with already determined volume of the acid solution in a 250 ml bottomed flask. The flask and its contents were heat-

ed to a fixed temperature of 70^{0}C while on a magnetic stirring plate and stirring was continued throughout the reaction duration. After the reaction time was completed, the suspension was immediately filtered to separate un-dissolved materials, washed three times with distilled water. The filtrate and washings were continued to a constant volume of 250 ml in a volumetric flask. The resulting solutions were diluted and analyzed for aluminum, magnesium, iron, calcium, sodium, and potassium ions using MS Atomic Absorption Spectrophotometer. The residue was also collected, washed to neutrality with distilled water, air dried and oven dried at 60^{0}C and labeled as UG0, UG2, UG4, UG8, UG12, UG14, and UG16, where the numbers denote the acid concentration used in the activation process. To study the kinetics of the dissolution process of the octahedral ions- aluminium, magnesium, and iron, the activation was repeated at different time ranges of 2 to 20 hours and temperatures of 60, 80, 90, and 100 ^{0}C.

2.2 Characterization

The chemical and mineralogical compositions of the natural and activated clay samples were determined. The chemical composition was determined using X-ray fluorescence (XRF), Philips PW 2400 XRF spectrometer; while the mineralogical composition was determined using Fourier transform infrared (FTIR), Shimadzu S8400 spectrophotometer, with samples prepared by the conventional KBr disc method. The surface area and cation exchange capacity of the treated and untreated samples were also determined in the following outlined methods:

2.3 Specific surface area

The surface area was determined using ethylene glycol mono-ethyl-ether (EGME) described by Carter et al (1965 and 1964). Clay samples were sun-dried and grinded to pass No. 40 sieve. A small amount of the sample was then placed in an oven at a temperature of 105 ^{0}C overnight to remove water and then dried with P_2O_5. One gram of the dried sample was spread into the bottom of aluminium tare and weighed (W_a) using an analytical balance with an accuracy of 0.001 g. Approximately 3.0 ml of laboratory grade EGME was added to the sample using a pipette and mixed together with a gentle swirling motion to create uniform slurry. All clay samples were covered with the EGME in order to obtain an accurate surface area measurement. The aluminium tare was then placed inside a standard laboratory glass sealed vacuum desiccator and allowed to equilibrate for 20 min. The desiccator was then evacuated using vacuum pump. The aluminium tare was removed from the desiccator and weighed (W_s) after a period of 12, 16, and 24 hours. When the mass of the sample varied by more than 0.001 grams between two measurements, the sample was placed back in the desiccator and evacuated again for an additional 2 hours. The process was continued until the sample mass did not vary by more than 0.001 g. The surface area was expressed as follows:

$$A = \frac{Wa}{0.000286Ws} \quad (1)$$

Where A = surface area, W_a = weight of EGME retained by the sample, W_s = weight of P_2O_5-dried sample, 0.000286 is the weight of EGME required to form uni-molecular layer on a square meter of the surface (Chiou et al, 1993).

2.4 Cation Exchange Capacity (CEC) (Ingelthorpe et al, 1993)

5 g of the clay sample was weighed into the 250 ml polythene bottle with a magnetic stirrer. The bottle and its contents were weighed (M_1). 100 ml of buffered barium chloride solution was added to the bottle and was placed on a magnetic stirring plate and agitated for 1 hour. At the end of the period, the bottle was centrifuged at 1500 rpm for 15 minutes and the supernatant was discarded. Further 200 ml of the buffered barium chloride solution was added and the mixture was agitated on a magnetic stirring plate for another 1 hour. The bottle and its contents were left overnight. The following day, the bottle and its contents were centrifuged at 1500 rpm for 15 minutes and the supernatant discarded. 200 ml of distilled water was added and agitated for few minutes on the magnetic stirring plate. It was centrifuged for further 15 minutes and the supernatant discarded. The bottle and its contents were weighed *(M_2)*. 100 ml of $MgSO_4$ solution was pipette into the bottle and stirred well and was left to stand for 2 hours with occasional agitation on the magnetic stirring plate. After 2 hours the contents were centrifuged at 1500 rpm for 15 minutes and the supernatant decanted into the stoppered bottle. 5 ml aliquot of this solution was pipette into a 100 ml conical beaker and 5 ml of ammonia buffer and 6 drops of indicator were added to it. This mixture was titrated with standard EDTA (titer A_1 ml). Another titration was done with a 5 ml of aliquot of 0.05 M $MgSO_4$ solution (titer B ml). The end point was indicated by a blue to pink colour change. The Cation Exchange Capacity was calculated as follows:

$$CEC = 8\left\{B - \frac{(A_1 x (100 + M_2 - M_1))}{100}\right\} meg/100g \quad (2)$$

Where M_1 = weight of bottle plus dry content (g), M_2 = weight of bottle plus wet content (g), A_1 = titration end-point of sample (ml), and B = titration end-point of $MgSO_4$ solution (ml)

2.5 Adsorption Capacity Study

To investigate the adsorption capacity of the activated clay samples, they were used to bleach soya bean oil. The method has been presented in earlier publication (Ajemba and Onukwuli, 2012).

3. Results and Discussions

3.1 Characterization

The chemical compositions of the liquid filtrates after acid activation are shown in Table 1. The removal of the dioctahedral cations depends on their form and amount within the bentonite sample. They are present in small quantity as exchangeable cations. It was observed that Ca^{2+} was easily removed more than the others of Na^{+} and K^{+}. It has been reported by researchers that Calcium ion occur as calcite which dissolves easily in acid medium, while the Na and K ions are present as feldspars that are resistant to acid attack (Dias et al., 2003; Motlagh et al., 2008; Temuujin et al., 2004). The removal of the tri-octahedral cations of Al^{3+}, Fe^{3+}, and Mg^{2+}, was observed to be dependent on the intensity of the acid attack, their removal increased as the acid concentration was increased until 14mol/l, and thereafter their removal decreased as the concentration increased to 16mol/l. The Mg^{2+} was easily removed at strong treatment of the acid reaching 85.9% at 14mol/l for 20 hours. The removal of Al^{3+} and Fe^{3+} were both slow with Fe^{3+} having faster removal rate at the same treatment. This is in agreement with the findings of other authors (Vincente et al, 1995).

Table 1. *Analysis of the filtrate: Percentage of cations removed by the different acid treatments, in relation to their content in the untreated bentonite, expressed in oxide form.*

Acid concentration (mol/L)	Time(h)	Chemical composition (%)					
		Al_2O_3	Fe_2O_3	MgO	Na_2O	CaO	K_2O
2	2	2.4	4.7	8.5	20.6	74.5	6.5
	4	5.7	9.5	12.7	25.3	78.3	14.9
	8	8.3	14.5	18.6	27.9	81.5	22.7
	12	11.2	17.8	22.5	29.9	84.2	28.5
	16	13.9	21.3	27.3	32.2	86.1	33.6
	20	14.3	29.4	35.9	33.1	87.2	37.3
4	2	3.9	7.5	13.1	23.5	76.6	10.4
	4	6.1	13.3	17.2	28.4	80.4	19.3
	8	9.8	19.2	23.3	32.4	83.3	26.7
	12	12.9	23.4	28.7	34.8	85.5	32.8
	16	14.8	28.7	32.8	36.5	87.3	38.5
	20	16.1	33.6	39.4	40.4	88.7	42.6
8	2	5.9	9.6	17.4	25.2	78.5	13.4
	4	7.7	15.8	23.1	30.2	83.4	22.5
	8	10.5	24.4	29.5	34.8	85.6	30.6
	12	13.7	30.1	36.2	39.7	87.2	37.3
	16	15.7	35.3	40.4	41.6	88.8	41.4
	20	18.4	39.4	46.9	43.8	89.7	44.9
12	2	7.6	11.4	22.3	28.7	80.5	17.2
	4	9.4	18.5	28.6	33.3	84.9	25.5
	8	12.4	27.5	35.2	37.6	86.8	34.9
	12	15.8	36.5	44.2	42.5	88.7	40.3
	16	18.8	41.4	53.9	46.1	89.6	45.1
	20	21.4	47.8	59.3	47.9	91.5	49.4
14	2	11.6	14.7	37.4	32.4	82.6	20.5
	4	14.7	22.6	46.3	35.6	86.5	29.3
	8	18.4	33.4	53.8	41.4	87.6	39.8
	12	24.9	40.1	62.2	46.3	89.8	44.6
	16	33.8	47.2	78.5	49.5	90.6	50.2
	20	42.9	54.3	85.9	52.6	92.6	56.7

16	2	9.2	12.9	24.8	34.6	84.2	23.8
	4	11.1	20.3	31.7	38.9	87.7	34.9
	8	13.4	30.7	39.7	44.7	88.9	43.6
	12	17.3	38.6	48.5	49.5	90.2	48.7
	16	22.8	44.9	59.8	53.4	91.9	54.8
	20	28.5	50.4	68.7	56.2	93.8	63.4

The content of SiO_2 was observed to increase as the acid concentration increased to 14mol/l and decreased with further increase in concentration (Table 2) and this could be due to the formation of mullite which protects the clay layers from further acid attack. The results of the chemical analysis of the solid residue are shown in Table 2. It was observed from Table 2 that as the acid concentration increased, the rate of the removal of the cations (Al^{3+}, Fe^{3+}, and Mg^{2+}) increased simultaneously. But, a maximum was reached at activation with 14mol/l HNO_3 above which the removal rate decreased with increase in the acid intensity. The behaviour shown by the Al^{3+}, Fe^{3+}, and Mg^{2+} (Table 2) contents with progressive acid treatment is related to the progressive dissolution of the clay mineral. The octahedral sheet destruction passes the cations into the solution, while the silica generated by the tetrahedral sheet remains in the solid phase due to its insolubility (Dias et al, 2003). Pesquera et al (1992) suggest that this free silica generated by the initial destruction of the tetrahedral sheet, is polymerized by the effect of such high acid concentration and is deposited on the undestroyed silicate fractions, thereby protecting it from further acid attack (Vicente-Rogriguez et al, 1994a and 1994b; Srasra et al, 1989). The analysis of the results shows a decrease in relative amount of cations belonging to octahedral sheet and an increase in the Si/ [Al + Fe + Mg] ratio (Table 2). This chemical change that took place in the clay structure during acid activation led to vacancies in the crystal lattice, and this increases the adsorptive power of the activated clay mineral. During the activation process, the protons of nitric acid replaces the exchangeable cations such as Na^+, K^+ and Ca^{2+} which are present between the layers. However, the protons of nitric acid cannot occupy all the empty spaces left by ions such as Al^{3+} and Mg^{2+} that occupy the octahedral sheet, thereby leaving some vacancies.

Table 2. *Chemical analysis of the natural and acid activated Ughelli bentonite samples determined by x-ray fluorescence (XRF) (Ajemba, 2012)*

Clay samples	Chemical composition (%)									Si/[Al + Fe + Mg]
	Al_2O_3	SiO_2	Fe_2O_3	MgO	Na_2O	K_2O	TiO_2	LOI	Total	
UG0	24.54	52.3	10.8	3.78	0.96	0.61	2.56	4.27	99.82	1.34
UG2	19.56	60.73	7.26	2.06	0.55	0.43	1.43	3.42	98.05	2.10
UG4	16.21	64.96	4.94	1.15	0.31	0.28	1.05	2.86	92.77	2.91
UG8	12.37	68.41	2.83	0.74	0.28	0.19	0.82	1.94	87.89	4.29
UG12	8.78	73.81	2.06	0.37	0.12	0.11	0.71	0.84	84.12	6.58
UG14	5.26	76.93	1.12	0.08	0.07	0.06	0.48	0.73	79.57	11.91
UG16	6.45	75.27	1.68	0.14	0.07	0.06	0.43	0.92	78.24	9.10

3.2 Surface area and Cation exchange capacity (CEC)

The results of the surface area and cation exchange capacity of the natural and activated samples are presented in Table 3. The data shows that the surface area increased as the intensity of the acid treatment increased until 10mol/l and thereafter decreased with further increase in the intensity. The surface area of the natural bentonite is 117.6m^2/g, and increased with mild acid treatments, reaching maximum value of 364m^2/g when treated with 14mol/l of HNO_3. It decreased with more intense treatment of HNO_3 to 325m^2/g; similar results were reported by others (Vicente Rodriguez et al, 1995; Suquet et al, 1992; Thompson et al, 1992). Analysis of the cation exchange capacity showed a decrease in its value as the acid concentration increased (Table 3). With the increase of concentration of HNO_3, the samples showed a gradual decrease of the CEC until treatment with 14mol/l acid. In treatment with 16mol/l HNO_3 acid, as the SiO_2 content decreased (Table 2), an increase of CEC was observed in comparison with the CEC of samples treated with 14mol/l. Tomic et al, (2011) reported similar result when they investigated the structural modification of sulphuric acid activated smectites.

Table 3. *Surface area and CEC of natural and nitric acid activated bentonite.*

Clay Samples	CEC (meq/100g)	Surface area (m^2/g)
UG0	186	117.6
UG2	138	187
UG4	104	243
UG8	85	284
UG12	79	318
UG14	48	364
UG16	58	325

3.3 Fourier transforms infrared (FTIR) spectroscopy analysis

The FTIR spectra of the raw and acid-leached clay samples were carried out in the range from 400 – 4000 cm^{-1} to study the effect of acid-leaching on the clay mineral. The FTIR spectra of the raw and acid-leached samples are shown in Figs 1 and 2, respectively. The changes in the functional groups provide the indication of the modifications that occurred during the activation process. During the acid-leaching of the clay samples the protons from the acid medium penetrate into the clay structures attacking the OH groups thereby causing the alteration in the adsorption bands attributed to the OH vibrations and octahedral cations. The intensities of the stretching bands observed at 3623, 3432, 1641, and 920 cm^{-1} (associated with O-H, along with Al-OH stretch) decreased after acid-activation. The increase in the severity of acid caused the disappearance of the stretching bands at 4660, 3694, 2376, and 998 cm^{-1} assigned to the H-O-H stretching. The peak assigned to Si-O-Si stretch at 788 and 1066 cm^{-1} remained after acid leaching, similar result was reported by others [Christidis et al., 1997; Komadel and Madejova, 2006]. The bands at 525, 690, and 998 cm^{-1} associated to Si-O-Al vibration disappeared after the acid treatment of the clay sample. The transformation of the tetrahedral occurred at 788 cm^{-1} which was increased after the acid treatment.

Fig.1. *FT-IR spectra of natural Ughelli bentonite (Ajemba, 2012).*

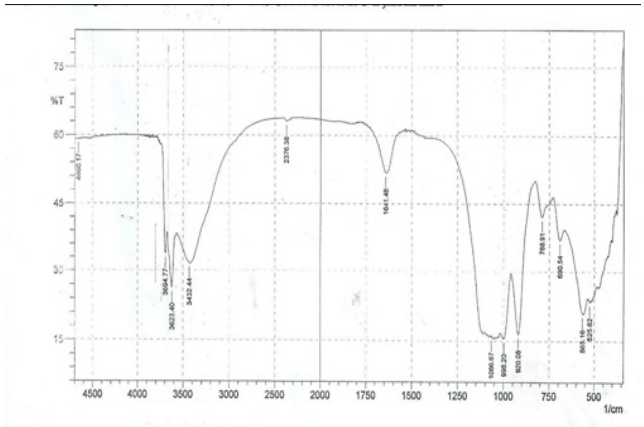

Fig.2. *FT-IR spectra of acid-activated Ughelli bentonite (Ajemba, 2012).*

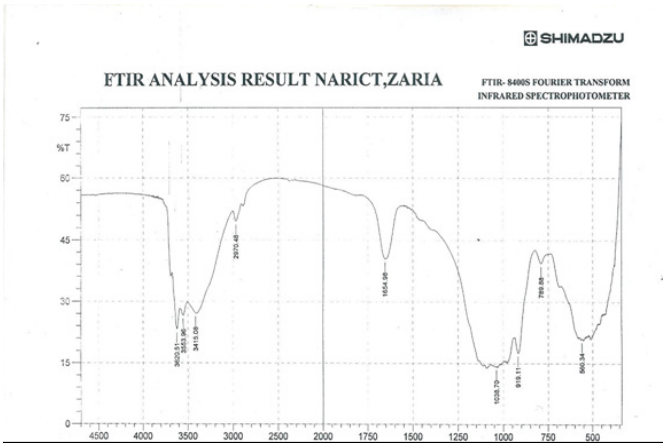

3.4 Activation kinetics Studies

The reaction between a solid and a fluid may be represented by

A (fluid) + b B (solid) --> Products (3)

The rate of reaction between a solid and a fluid can be expressed by heterogeneous and homogeneous reaction models. According to the shrinking-core model, the reaction is considered to take place at the outer surface of the unreacted particle. When no ash forms, the reacting particle shrinks during reaction, and finally disappears. For a reaction of this kind, the following three steps are considered to occur in succession during reaction (Levenspiel, 1972).

1. Diffusion of fluid reactant through the fluid layer to the surface of the solid.
2. Reaction of the fluid reactant and solid on the surface of the solid.
3. Diffusion of the products through the film layer to the bulk fluid.

The slowest of these sequenced steps is the rate-determining step. If the reaction is controlled by film diffusion, it becomes

$$X = [3bk_cC_A / \rho_B R]\, t = k_f t \quad (4)$$

If it is controlled by chemical reaction, it becomes

$$1 - (1 - X)^{1/3} = [bk_sC_A / \rho_B R]\, t = k_r t \quad (5)$$

The product layer diffusion control is given by

$$1+2(1-X)-3(1- X)^{2/3} = [2M_BDC_A/\rho_B bR^2]\, t = k_d t \quad (6)$$

The experimental data were tested with the above kinetic

models, and it was determined statistically that the dissolution reaction fitted the chemical reaction (Eq. (5)) model. The plots are shown in Figures 3 to 5.

Fig.3. *Plot of 1 – (1 – X) $^{1/3}$ versus time for the removal of Al^{3+} from bentonite samples activated with different acid concentrations.*

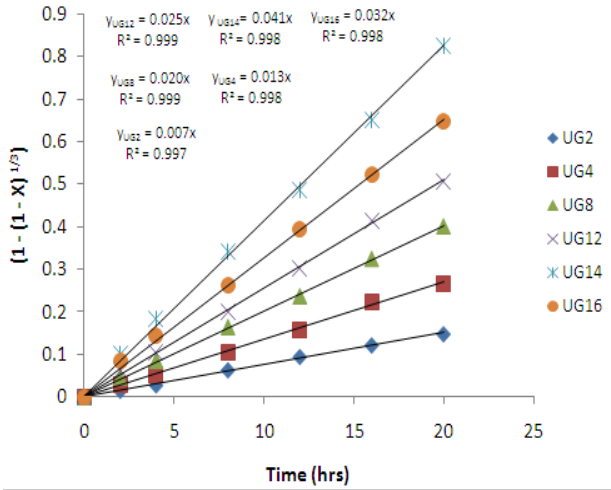

Fig.4. *Plot of 1 – (1 – X) $^{1/3}$ versus time for the removal of Fe^{3+} from bentonite samples activated with different acid concentrations.*

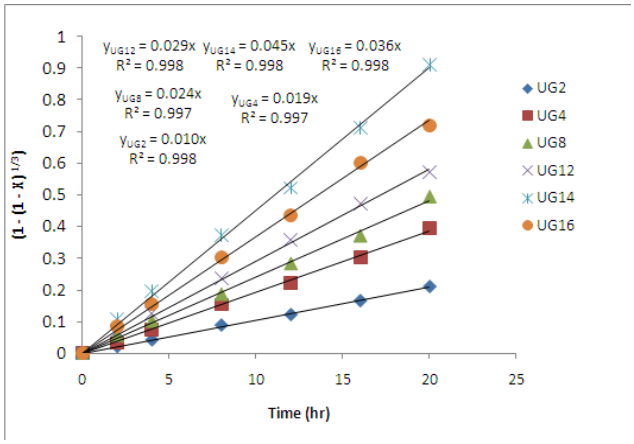

Fig.5. *Plot of 1 – (1 – X) 1/3 versus time for the removal of Mg2+ from bentonite samples activated with different acid concentrations.*

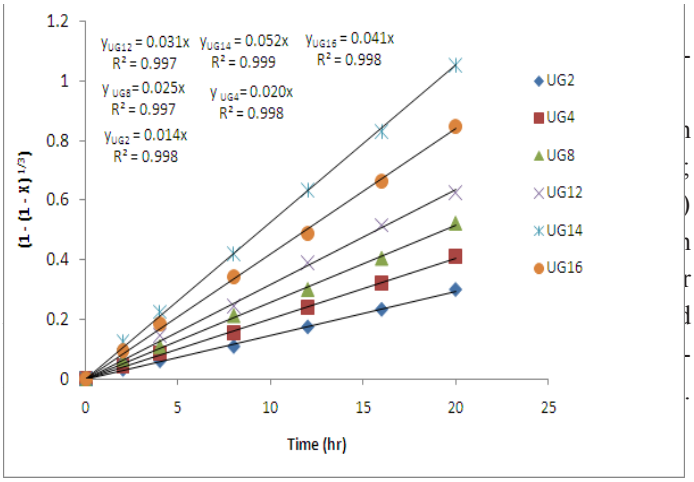

3.5 Effect of temperature on activation

The effect of temperature on the rate of activation was investigated at 60, 80, 90, and 100 ^{0}C. The analysis shows that the activation rate has a linear relationship with the temperature as shown in Figure 6. The data of Figure 6 were fitted to the chemical reaction model and the data conformed to it and it is shown in Figure 7. The activation was observed to reach 55% at 100^{0}C. This shows that the reaction is endothermic. At high temperature collision of the particles and the liquid molecules is enhanced. The relationship between the overall reaction rate constant and temperature according to the Arrhenius equation was employed in calculating the activation energy. The slope of the plot of Arrhenius equation was used to calculate the activation energy to be 39.009kJ/mol.

Fig.6. *Plot of the fraction of cations removed from the 14mol/l activated Ughelli bentonite at different temperatures.*

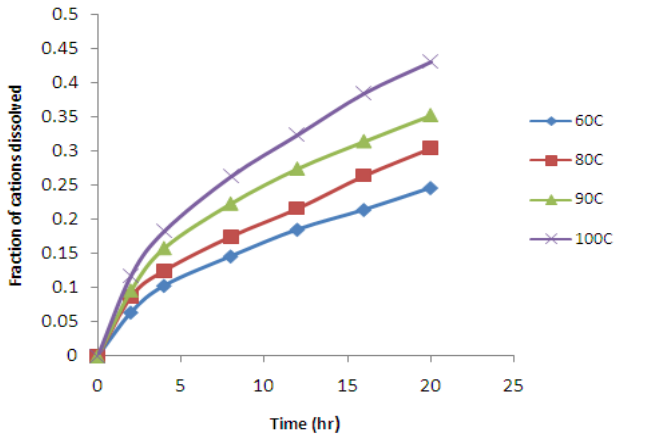

Fig.7. *Plot of 1 – (1 – X) $^{1/3}$ versus time for cations removal at different temperatures.*

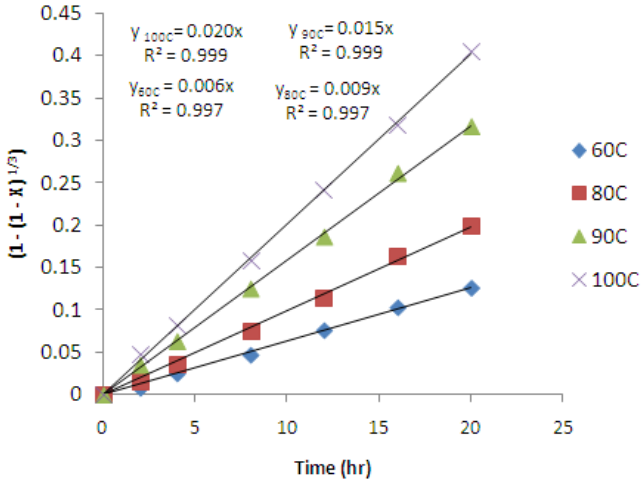

3.6 Adsorption studies

To investigate the adsorptive performance of the acid treated samples, the samples were used to adsorb colour pigments from soybean oil and the results are presented in Figure 8. The figure

shows that the adsorption power increased gradually as the intensity of the acid treatment increased and reached a maximum with 14mol/l treated sample. Further increased in the intensity of treatment to 16mol/l caused a reduction in the adsorption capacity and this could be as a result of destruction of the bentonite crystalline structure, reduced surface area and Si/ [Al + Fe + Mg] ratio (Tables 2 and 3).

Fig.8. *Plot of the bleaching efficiencies of the natural and activated bentonite samples.*

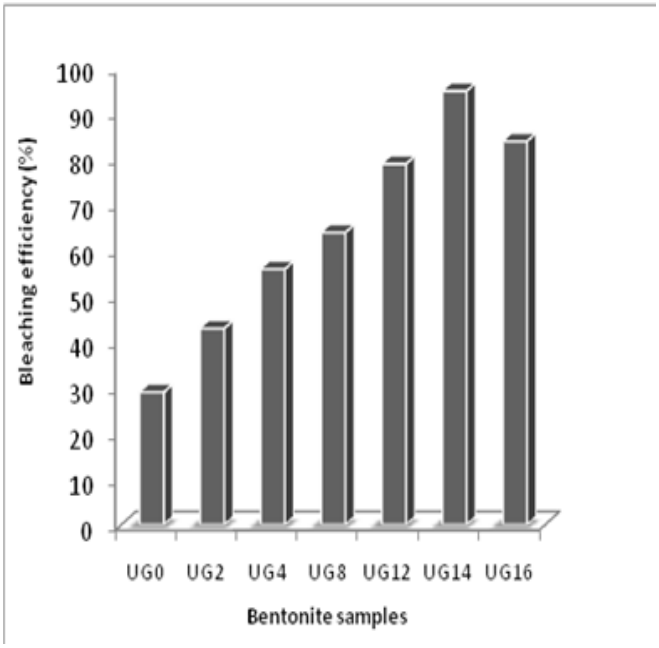

4. Conclusions

Alteration of the bentonite structure by acid treatment has been investigated in this study. Analyses of the results showed that the acid treatment resulted in re-organization of the structure by the leaching out of the octahedral cations from the clay sheet and creation of vacant sites. The kinetic study revealed that the activation process is controlled by the chemical reaction of the acid and the bentonite molecules with activation energy of 39.009kJ/mol. The chemical and physical properties of the modified samples were observed to have increased after activation. Such properties include: surface area, cation exchange capacity, and adsorption capacity. The present study has revealed the possibility of using Ughelli bentonite as bleaching earth in the vegetable oil industry.

5. References

1. Abdul-Latif N and Weaver C (1969) Kinetics of acid dissolution of palygorskite (attapulgite) and sepiolite. Clays Clay Miner., 17, 169 – 174.
2. Ajemba RO (2012) Thermodynamics and kinetics studies of the dissolution and adsorptive applications of Ukpor, Udi, and Nteje clays. Ph.D. Thesis, Nnamdi Azikiwe University, Nigeria.
3. Ajemba RO and Onukwuli OD (2012) Evaluation of the effects of acid activation on adsorptive properties of clay from Ukpor in bleaching palm oil. Int. J. Multi. Sci. Eng. 3 (5), 46.
4. Amari A, Chlendi M, Gannouni A, and Bellagi A (2010) Optimised activation of bentonite for toluene adsorption, Appl. Clay Sci. 47, 457 – 461.
5. Bergaya F and Lagaly G (2001) Surface modification of clay minerals. Appl. Clay Sci. 19, 1 – 3.
6. Boki K, Kudo M, Wada T and Tamura T (1992) Bleaching of alkali-refined vegetable oils with clay minerals. J. Am. Oil Chem. Soc., v. 69, 232 – 236.
7. Breen C, Zahoor ED, Madejova J and Komadel P (1997) Characterization and catalytic activity of acid-treated, size-fractionated smectites. J. Phys. Chem., B. v. 101, 5324 – 5331.
8. Carrado KA and Komadel P (2009) Acid activation of bentonite and polymer-clay nanocomposites. Elements, 5, 111 – 116.
9. Carter DL, Heilman MD, and Gonzalez CL (1965) Ethylene Glycol Mono-ethyl Ether for determining surface area of silicate minerals, Soil Sci., 100, 356 – 361.
10. Carter DL, Mortland MM and Kemper WD (1964) Specific surface. Methods of soil analysis, Chapter 16, Agronomy, No. 9, Part 1, 2nd Ed., American Society of Agronomy, 456.
11. Chiou CT, Rutherford DW and Manes M (1993) Sorption of N_2 and EGME vapours on some soils, clays, and mineral oxides and determination of sample surface areas by use of sorption data, Environ. Sci. Technol., 27, 1587 – 1591.
12. Christidis GE, Scott PW and Dumham AC (1997) Acid activation and bleaching capacity of bentonites from the islands of Milos and Chios, Aegean and Greece, Appl. Clay Sci. 12, 329 – 347.
13. Corma A, Mifsud A and Perez J (1986) Etude cietique de l'attaque acide de la sepiolite: Modifications des proprieties texturales, Clay Min., 21, 69 – 84.
14. Dias MI Suarez MB, Prates S and MartinPozas JM (2003) Characterization and acid activation of Portuguese special clays, Clay Min., 38, 537 – 533.
15. Fahn R and Fenderl K (1983) Reaction products of inorganic dye molecules with acid treated montmorillonite, Clay Min., 18, 447 – 452.
16. Falaras P, Kovanis I, Lezou F and Seiragakis G (1999) Cotton seed oil bleaching by acid-activated montmorillonite. Clay Miner. 34, 221 – 232.
17. Inglethorpe SDJ, Morgan DJ, Highley DE and Bloodworth AJ (1993) Industrial mineral laboratory manual- Bentonite, British Geological Survey Technical Report, WG/93/20.

18. Kheok SC and Lim EE (1982) Mechanism of palm oil bleaching by montmorillonite clay activated at various acid concentrations. J. Am. Oil Chem. Soc. 59, 129 – 131.

19. Komadel P (2003) Chemically modified smectites, Clay Min. 38, 127 – 138.

20. Komadel P and Madejova J (2006) Acid activation of clay minerals. In Handbook of Clay Science, edited by F. Bergaya; B. K. Theng and G. Lagaly. Development in Clay Science, Vol. 1, Elsevier Ltd.

21. Komandel P, Schmidt D, Medejova J and Cicel J (1990) Alteration of smectites by treatment with hydrochloric acid and sodium carbonate solutions. Appl. Clay Sci. 5, 113 – 122.

22. Levenspiel O (1972) Chemical Reaction Engineering, 2nd edition; John Wiley and Sons: New York.

23. Madejova J, Budjak J, Janek M and Komadel P (1998) Comparative FTIR study of structural modifications during acid treatment of dioctahedral smectite and hectorite. Spectrochimica Acta. Part A, 54, 1397 – 1406.

24. Madejova J, Pentrak M, Palkova H and Komadel P (2009) Near infrared spectroscopy: a powerful tool in studies of acid treated clay minerals. Vib. Spectro. 49, 211 – 218.

25. Mokaya R and Jones W (1995) Pillared clays and pillared acid-activated clays: A comparative study of physical, acidic and catalytic properties, J. Porous Mat. 6, 335.

26. Morgan DA, Shaw DB, Sidebottom TC, Soon TC and Taylor RS (1985) The function of bleaching earth in the processing of palm, palm kernel and coconut oils. J. Am. Oil Chem. Soc., 62, 292 – 299.

27. Motlagh MM, Rigi ZA and Yuzbashi AA (2008) To evaluate an acid activated bentonite from Khorasan (Iran) for use as bleaching clay, Int. J. Eng. Sci., 19, 83 – 87.

28. Osthaus BB (1954) Chemical determination of tetrahedral ions in nontronite and montmorillonite. Clays Clay Min. 2, 404 – 409.

29. Osthaus BB (1956) Kinetics studies on montmorillonite and nontronite by the acid dissolution technique, Clays Clay Min. 4, 301 – 307.

30. Pesquera C, Gonzalez F, Benito I, Blanco C, Mendioroz S and Pajares J (1992) Passivation of a montmorillonite by the silica created in acid activation, J. Mat. Chem., 2, 907 – 912.

31. Rhodes CN and Brown DR (1992) Structural characterization and optimization of acid treated montmorillonite and high porosity silica supports for $ZnCl_2$ alkylation catalysts. J. Chem. Soc. Faraday Trans. 88, 2269 – 2274.

32. Srasra E, Bergaya F, Vandammne H and Arigub NK (1989) Surface properties of an activated bentonite: Decolourization of rape-seed oils, Appl. Clay Sci., 4, 411 – 418.

33. Suquet H, Chevalier S, Marcilly C and Barthomeuf D (1992) Preparation of porous materials by chemical activation of Llanovermiculite, Clays Clay Min., 26, 49 – 60.

34. Taha KK, Suleiman TM and Musa AM (2011) Performance of Sudanese activated bentonite in bleaching cotton seed oil, J. Bangladesh Chem. Soc., 24 (2), 191 – 201.

35. Taylor DR, Jenkins DB and Ungermann CB (1989) Bleaching with alternative layered minerals: a comparison with acid activated montmorillonite for bleaching soybean oil. J. Am. Oil Chem. Soc., 66, 334 – 341.

36. Temuujin J, Jadamobaa T, Burmaa G, Erdenechimeg S, Amarsanaa J and Mackenzie KJD (2004) Characterization of acid activated montmorillonite from Tuulant (Mongolia), Ceram. Int., 30, 251 – 253.

37. Thompson JG, Uwins PJR, Whittaker AK and Mackinnon IDR (1992) Structural characterization of Kaolinite: NaCl intercalate and its derivatives, Clays Clay Min., 40, 369 – 380.

38. Tomic PZ, Antic Mladenovic SB, Babic BM, Poharc Logar VA, Dordevic AR and Cupac SB (2011) Modification of smectite structure by sulphuric acid and characteristics of the modified smectite. J. Agric. Sci., 56 (1), 25 – 35.

39. Tyagi B, Chudasama CD and Jasra RV (2006) Determination of structural modification in acid activated montmorillonite clay by FTIR spectroscopy. Spectrochimica Acta Part A, 64, 273 – 278.

40. Vicente-Rodriguez MA, Lopez-Gonzalez JD and Banares-Munoz MA (1994a) Acid activation of a Spanish sepiolite: Physico-chemical characterization, free silica content and surface area of the solids obtained, Clay Min., 29, 361 – 368.

41. Vicente-Rodriguez MA, Lopez-Gonzalez JD, Banares-Munoz MA and Casado-Linarejos J (1995) Acid activation of Spanish sepiolite II. Consideration of kinetics and physico-chemical modifications generated, Clay Min., 30, 315 – 321.

42. Vicente-Rodriguez MA, Suarez-Barrios M, Lopez-Gonzalez JD and Banares-Munoz MA (1994b) Acid activation of a ferrous saponite (griffithite): Physico-chemical characterization and surface area of the products obtained, Clays Clay Min., 42, 724 – 731.

43. Vicente Rodriguez MA, Suarez M, Lopez Gonzalez JD and Banares Munoz MA (1996) Characterization, surface area and porosity analyses of the solids obtained by acid leaching of a saponite, Langmuir, 12, 566 – 572.